

Analysis of a Nonlinear Sampled-data Proportional Navigation System Having Adjustable Parameters

by TAIN-SOU TSAI

Institute of Electronics, National Chiao Tung University, Hsinchu, Taiwan, Republic of China

and KUANG-WEI HAN

Chung-Shan Institute of Science and Technology, Lung Tan, Taiwan, Republic of China

ABSTRACT: *The proportional navigation system analysed in this paper is a complicated nonlinear sampled-data control system. The stability boundaries and limit cycles of the system are found by the stability-equation method. The results obtained are useful for analysing the tracking characteristics of the system, especially in the nonlinear region for which no analysis is given in the current literature.*

Nomenclature

A, A_1	sinusoidal input at the input of nonlinearity
N	navigation constant
$N_1(A_1), N_2(A)$	describing functions of the nonlinearity
$p(t)$	geometry relation
S	Laplace operator
W	operator in W -domain
ω	frequency in S -domain
v	frequency in W -domain
T	sampling period
Z	operator in Z -domain
α, β	parameters
ρ	damping ratio

1. Introduction

The navigation system shown in Fig. 1 is a homing system for engaging a moving target in the vertical plane (1). The seeker is a microwave or an infrared device. In general, there are many nonlinearities in this system, but in this work only two evident nonlinearities, i.e. the truncated sine function in the seeker and the backlash in the servo, are considered.

For analysis, the stability-equation method (2), is used. The results of the analysis

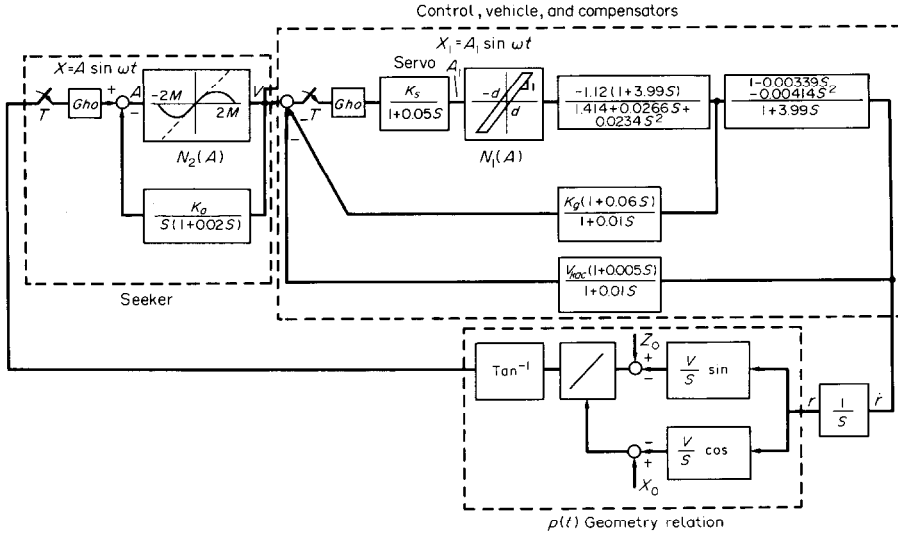


FIG. 1. Block diagram of a proportional navigation system.

will show that the characteristics of the system, such as the asymptotically stable region, limit cycle region and unstable region can be clearly found.

In the current literature for such a complicated system, the analysis is usually confined to the linear region of the seeker, i.e. to approximate the sine function by a linear gain (3) and then to study the effects of nonlinearities and adjustable parameters by use of computer simulation. However, in this paper, analytical results are presented which can let the engineer have a thorough understanding of the system considered, especially the effects due to nonlinearities.

II. Analysis of the Linear Continuous-data System

For comparative purposes, the linear model of the system considered with continuous-data is analysed in this section. Assume that the nonlinearities are replaced by unit gains and the samplers are closed at all times without the holding devices, then the transfer function of the seeker becomes

$$\frac{V_r(S)}{\sigma(S)} = \frac{N_2(A)S(1+0.02S)}{N_a N_2(A) + S(1+0.02S)} \tag{1}$$

The combined transfer function of the control system and the vehicle dynamics is

$$\begin{aligned} \frac{\dot{r}}{V_r(S)} = & -1.12K_s(1+0.01S)(1-0.00339S-0.00414S^2)/ \\ & [(1+0.01S)(1+0.05S)(1.414+0.0266S+0.0234S^2) \\ & -1.12K_sK_g(1+3.99S)(1+0.06S)-1.12K_sVK_{ac}(1-0.00339S \\ & -0.00414S^2)(1+0.005S)]. \end{aligned} \tag{2}$$

In order to ensure that the proportional navigation system has a navigation constant N , it is required that the steady state ratio of \dot{r} and $\dot{\sigma}$ be equal to (3)

$$\left[\frac{\dot{r}}{\dot{\sigma}} \right]_{ss} = \frac{-1.12K_s}{K_a(1.414 - 1.12K_sK_g - 1.12K_sVK_{ac})} = N. \tag{3}$$

Let

$$-1.12K_sK_g = \alpha \quad -1.12K_sVK_{ac} = \beta, \tag{4}$$

where α and β are two parameters, then Eq. (3) gives

$$-1.12K_s = NK_a(1.414 + \alpha + \beta). \tag{5}$$

Assume that the time variant geometry relation is replaced by $p(t)$ (3). Then the characteristic equation of this continuous-data system is

$$\begin{aligned} & 1 + \alpha \frac{N_1(A_1)(1 + 3.99S)(1 + 0.06S)}{(1 + 0.05S)(1.414 + 0.0266S + 0.0234S^2)(1 + 0.01S)} \\ & + \beta \frac{N_1(A_1)(1 - 0.00339S - 0.00414S^2)(1 + 0.005S)}{(1 + 0.05S)(1.414 + 0.0266S + 0.0234S^2)(1 + 0.01S)} \\ & - NK_a(1.414 + \alpha + \beta) \cdot \frac{N_1(A_1)(1 - 0.00339S - 0.00414S^2)}{S(1 + 0.05S)(1.414 + 0.0266S + 0.0234S^2)} \cdot p(t) \\ & \times \frac{N_2(A)S(1 + 0.02S)}{N_2(A)K_a + S(1 + 0.02S)} = 0. \end{aligned} \tag{6}$$

Equation (6) indicates that the condition for system stability is $p(t) \leq 1/N$ because Eq. (6) has a singularity ($S = 0$) at $p(t) = 1/N$ (3). The stability boundaries for $N_1(A_1) = 1$, $N_2(A) = 1$ and $K_a = 15$ can be found by use of the stability-equation method. The results are shown in Fig. 2. The general procedure is given in the

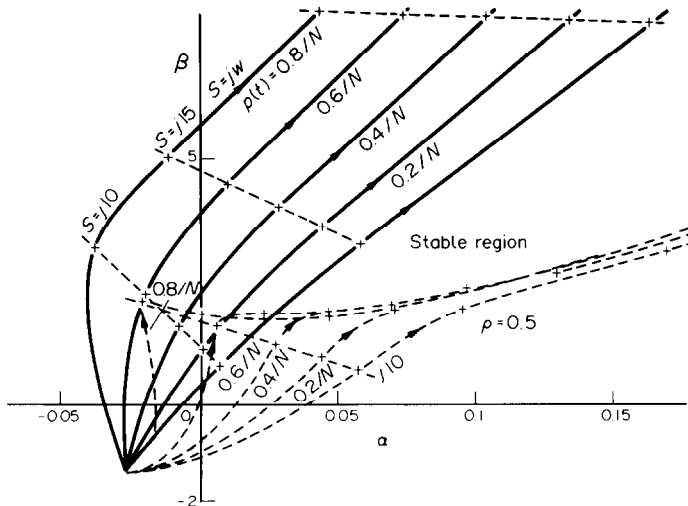


FIG. 2. Stability boundaries of a linear continuous-data control system.

Appendix where the detailed calculations are omitted. In Fig. 2, the regions below the constant $p(t)$ curves represent stable systems.

In Fig. 2, boundaries with damping ratio $\rho = 0.5$ are also shown (4). One may select a set of α and β for the desired damping characteristics of the system. Thus, the method is useful for design. Since the geometric relation $p(t)$ is time dependent, the stability boundaries of the system should be evaluated by considering various values of $p(t)$.

III. Analysis of the Linear Sampled-data System

Assume that the nonlinearities are replaced by unit gains, then the characteristic equation of the system is

$$\begin{aligned}
 & 1 + \left[Gho \cdot \frac{-1.12K_s K_g N_1(A_1)(1 + 3.99S)(1 + 0.06S)}{(1 + 0.05S)(1.414 + 0.0266S + 0.0234S^2)(1 + 0.01S)} \right]^* \\
 & + \left[Gho \cdot \frac{-1.12K_s V K_{ac} N_1(A_1)(1 - 0.00339S - 0.00414S^2)(1 + 0.005S)}{(1 + 0.05S)(1.414 + 0.0266S + 0.0234S^2)(1 + 0.01S)} \right]^* \\
 & - \left[Gho \cdot \frac{-1.12K_s N_1(A_1)(1 - 0.00339S - 0.00414S^2)}{S(1 + 0.05S)(1.414 + 0.0266S + 0.0234S^2)} \right]^* \cdot p(t) \\
 & \times \left[Gho \cdot \frac{N_2(A)S(1 + 0.02S)}{N_2(A)K_a + S(1 + 0.02S)} \right]^* = 0 \tag{7}
 \end{aligned}$$

where Gho is the zero-order holding device with transfer function $Gho = (1 - e^{-ST})/S$ and T is the sampling period.

Taking the Z -transformation of Eq. (7) for $T = 0.05$ sec, and using Eqs. (4) and (5), the characteristic equation can be found as

$$\begin{aligned}
 & 1 + \alpha \frac{N_1(A_1)(1.296 \times 10^{-6}Z^4 + 7.4668Z^3 - 8.9719Z^2 + 0.8598Z + 0.7079)}{(Z - 0.3679)(Z - 6.738 \times 10^{-3})(Z^2 - 1.7997Z + 0.9448)} \\
 & + \beta \frac{N_1(A_1)(-3.201 \times 10^{-5}Z^4 - 0.08902Z^3 + 0.2319Z^2 - 0.0717Z - 6.7359 \times 10^{-3})}{(Z - 0.3679)(Z - 6.738 \times 10^{-3})(Z^2 - 1.7997Z + 0.9448)} \\
 & - N_1(A_1)N_2(A)K_a Np(t)(1.414 + \alpha + \beta) \\
 & \times \frac{-3.001 \times 10^{-3}Z^4 + 0.005624Z^3 + 0.002708Z^2 - 2.1169 \times 10^{-3}Z + 1.414 \times 10^{-5}}{Z^2(Z - 0.3679)(Z^2 - 1.7997Z + 0.9448)} \\
 & \times \frac{Z^2 + a_4Z}{Z^2 + a_2Z + a_1} = 0 \tag{8a}
 \end{aligned}$$

where the values of a_1 , a_2 and a_4 are dependent on those of K_a and $N_2(A)$, i.e. one must evaluate the characteristic equation for each set of values of K_a and $N_2(A)$.

Taking the W -transformation of Eq. (8a) with $Z = (1 + w)/(1 - w)$, the charac-

teristic equation in the W -domain can be found as

$$\begin{aligned}
 & 1 + \alpha \frac{N_1(A_1)(13.217W^4 - 3.113W^3 + 4.306W^2 + 2.012W + 1.249 \times 10^{-2})}{W^4 + 1.478W^3 + 0.5374W^2 + 6.956 \times 10^{-2}W + 1.766 \times 10^{-2}} \\
 & + \beta \frac{N_1(A_1)(7.49 \times 10^{-2}W^4 + 1.1626 \times 10^{-2}W^3 - 9.738 \times 10^{-2}W^2 - 1.8097W + 1.256 \times 10^{-2})}{W^4 + 1.478W^3 + 0.5374W^2 + 6.956 \times 10^{-2}W + 1.766 \times 10^{-2}} \\
 & - N_1(A_1)N_2(A)K_a Np(t)(1.414 + \alpha + \beta) \\
 & - 7.392 \times 10^{-3}W^4 - 5.377 \times 10^{-3}W^3 - 4.556 \times 10^{-3}W^2 + 6.680 \times 10^{-4}W + 6.303 \times 10^{-4} \\
 & \times \frac{W^4 + 1.492W^3 + 0.544W^2 + 7.022 \times 10^{-2}W + 1.792 \times 10^{-2}}{W^4 + 1.492W^3 + 0.544W^2 + 7.022 \times 10^{-2}W + 1.792 \times 10^{-2}} \\
 & \times \frac{(1 - a_4)W^2 + 2W + a_4 + 1}{(1 - a_2 + a_1)W^2 - (2a_1 - 2)W + a_2 + a_1 + 1} = 0. \tag{8b}
 \end{aligned}$$

Applying the stability-equation method for $N_1(A_1) = 1$, $N_2(A) = 1$ and $K_a = 15$, the stability boundaries are found for each constant value of $p(t)$. The results are shown in Fig. 3.

For testing, a disturbance at the input of the seeker is assumed. The amplitude of the disturbance is equal to 0.3 and it is held for one sampling period ($T = 0.05$ sec), and the geometric relation $p(t)$ is set at $0.6/N$. In Fig. 3, four points (Q_1 - Q_4) are selected. After the corresponding values of α and β are substituted into the block diagram of the system shown in Fig. 1, the response of the system to the testing signal specified above can be obtained by computer simulation. The results are shown in Fig. 4, where A is the amplitude of the signal in front of the nonlinearity in the seeker. If $p(t)$ is set to be $0.6 \cos 25 t/N$ (for illustration only), the response due to the same

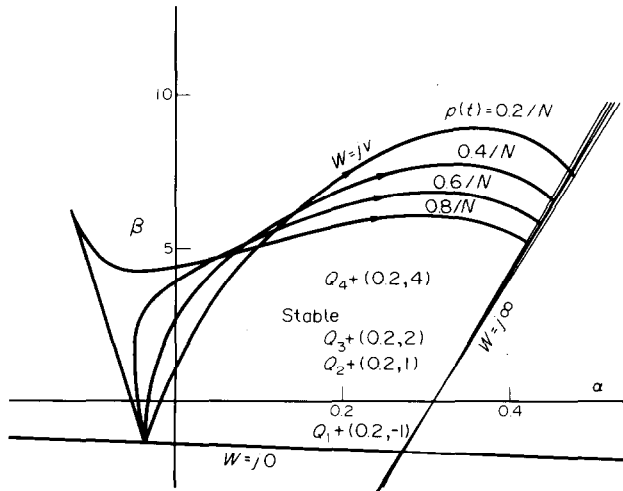


FIG. 3. Stability boundaries of a linear sampled-data control system.

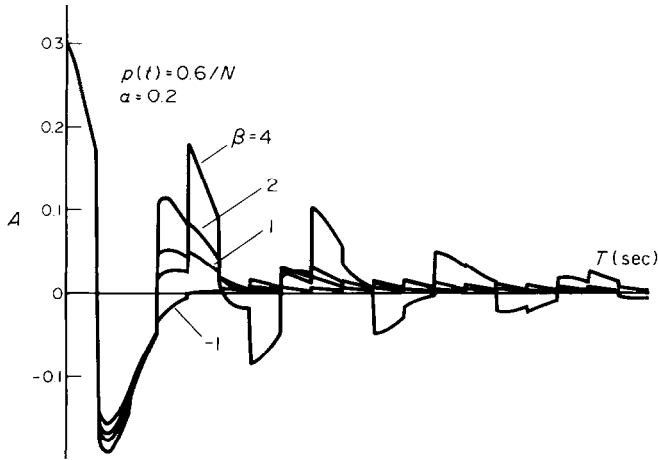


FIG. 4. Responses of a linear sampled-data control system to a testing signal.

distance can die out quickly as shown in Fig. 5. In other words, the system can engage the target quickly if the operating points are selected at any one of the four points in the stable region in Fig. 3. By use of computer simulation, it has been checked that any point outside the stability boundary will give an unstable system.

IV. Analysis of the Nonlinear Sampled-data System

For the nonlinearity in the seeker, the approximated sine function $y(x) = 2M \sin(\pi x/2M)/\pi$ is used, for which the describing function can be found as

$$N_2(A) = \begin{cases} b \int_0^\pi \sin(a \sin \theta) \sin \theta \, d\theta & A \leq 2M \\ 2b \int_0^r \sin(a \sin \theta) \sin \theta \, d\theta & A \geq 2M \end{cases} \tag{9a}$$

where $a = (\pi A)/(2M)$, $b = (4M)/(\pi^2 A)$, $r = \sin^{-1} [(2M/A)]$, and A is the amplitude of the sinusoidal input to the nonlinearity. The describing function of the backlash in $N_1(A_1) = g_1(A_1) + jb_1(A_1)$, where

$$g_1(A_1) = \frac{1}{\pi} \left\{ \frac{\pi}{2} + \sin^{-1} \left(1 - \frac{2d}{A_1} \right) + 2 \left(1 - \frac{2d}{A_1} \right) \left[\frac{d}{A_1} \left(1 - \frac{d}{A_1} \right) \right]^{1/2} \right\}$$

$$b_1(A_1) = -\frac{4d}{\pi A_1} \left(1 - \frac{d}{A_1} \right), \quad A_1 \geq d \tag{9b}$$

and A_1 is the amplitude of the sinusoidal input to the backlash.

If the nonlinearities are in a single loop or in a continuous-data system, the relationship between A and A_1 can be derived easily. But the nonlinearities of the system analysed are separated by samplers, and in two independent loops;

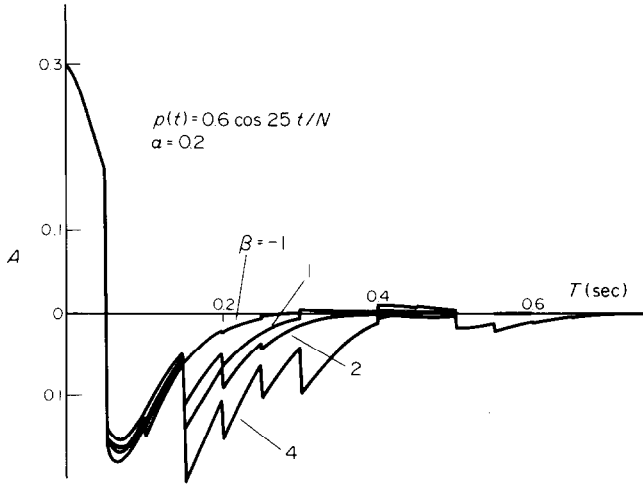


FIG. 5. Responses of a linear sampled-data control system to a testing signal.

therefore, further manipulations are required. It will be shown that the combination of an equivalent system and the characteristic equation will provide an effective way to analyse this nonlinear sampled-data system.

A symbolic block diagram of the system considered can be drawn as shown in Fig. 6(a), which gives

$$C(S)^* = \frac{[G_1(S)N_1(A_1)G_2(S)G_3(S)G_5(S)]^*}{1 + [G_1(S)N_1(A_1)G_2(S)G_6(S)]^*[G_1(S)N_1(A_1)G_2(S)G_7(S)]^*} R^*(S) \quad (10a)$$

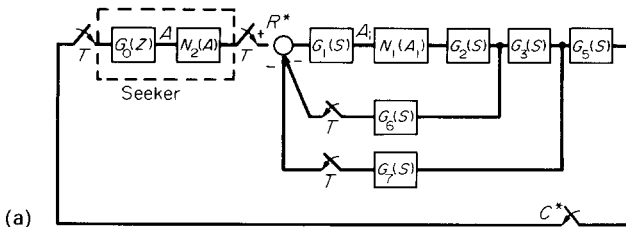


FIG. 6(a). Symbolic blocks of Fig. 1.

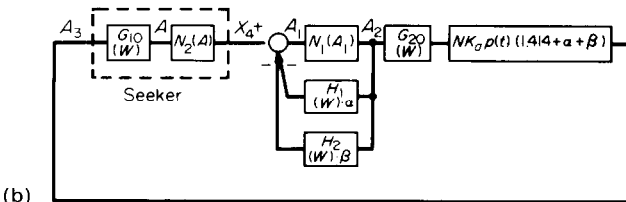


FIG. 6(b). Equivalent system of Fig. 1 in W-domain.

and

$$C(S)^* = \frac{N_1(A_1)[G_1(S)G_2(S)G_3(S)G_5(S)]^*}{1 + N_1(A_1)[G_1(S)G_2(S)G_6(S)]^* + N_1(A_1)[G_1(S)G_2(S)G_7(S)]^*} \cdot R^*(S) \quad (10b)$$

The equivalent system represented by Eq. (10) can be converted to the W -domain as shown in Fig. 6(b), where

$$\begin{aligned} \alpha H_1(W)|_{z=(1+w)/(1-w)} &= [G_1(S)G_2(S)G_6(S)]^*|_{S=1/T \ln z} \\ \beta H_2(W)|_{z=(1+w)/(1-w)} &= [G_1(S)G_2(S)G_7(S)]^*|_{S=1/T \ln z} \\ G_{20}(W)NK_a p(t)(1.414 + \alpha + \beta)|_{z=(1+w)/(1-w)} &= [G_1(S)G_2(S)G_3(S)G_5(S)]^*|_{S=1/T \ln z} \end{aligned} \quad (11)$$

Equation 11 is derived from the relationship of Eqs. (3) and (4). For a specified amplitude A or (A_2) and a specified frequency $w = jv$, one has

$$\begin{aligned} A_2 &= |g_1(A_1) + jb_1(A_1)| \cdot A_1 \\ A_3 &= K_a \cdot N \cdot p(t)(1.4 \cdot 4 + \alpha + \beta) \cdot |G_{20}(jv)| \cdot |g_1(A_1) + jb_1(A_1)| \cdot A_1 \\ X_4 &= N_1(A) \cdot |G_{10}(jv)| \cdot K_a \cdot N \cdot p(t)(1.414 + \alpha + \beta) \cdot |G_{20}(jv)| \cdot |g_1(A_1) + jb_1(A_1)| \cdot A_1. \end{aligned}$$

Since

$$\begin{aligned} A_1 &= X_4 - (\alpha |H_1(jv)| + \beta |H_2(jv)|) \cdot |g_1(A_1) + jb_1(A_1)| \cdot A_1 \\ X_4 &= A_1 + A_1(\alpha |H_1(jv)| + \beta |H_2(jv)|) |g_1(A_1) + jb_1(A_1)| \end{aligned}$$

one has

$$\begin{aligned} A_1 + A_1 |g_1(A_1) + jb_1(A_1)| \cdot \{\alpha |H_1(jv)| + \beta |H_2(jv)| - N_2(A) \cdot K_a N p(t) \\ \times (1.414 + \alpha + \beta) \cdot |G_{10}(jv)| \cdot |G_{20}(jv)|\} = 0. \end{aligned} \quad (12)$$

Equation (12) shows that the value of A (or A_1) depends on the frequency $w = jv$ and the parameters α and β .

The characteristic equation of the system can be found as

$$\begin{aligned} (W^4 + 1.478W^3 + 0.5374W^2 + 6.956 \times 10^{-2}W + 1.766 \times 10^{-2}) \\ \times [(1 - a_2 + a_1)W^2 + (2a_1 - 2)W + a_2 + a_1 + 1] + \alpha N_1(A_1) \\ \times (-3.127W^4 - 3.113W^3 + 4.306W^2 + 2.012W + 1.249 \times 10^{-2}) \\ \times [(1 - a_2 + a_1)W^2 + (2a_1 - 2)W + a_2 + a_1 + 1] + \beta N_1(A_1) \\ \times (7.49 \times 10^{-2}W^4 + 1.1626 \times 10^{-2}W^3 - 9.738 \times 10^{-2}W^2 \\ - 1.8097 \times 10^{-2}W + 1.256 \times 10^{-2}) [(1 - a_2 + a_1)W^2 + (2a_1 - 2)W \\ + a_2 + a_1 + 1] - N_1(A_1)N_2(A)K_a N p(t)(1.414 + \alpha + \beta) \\ \times (-7.392 \times 10^{-3}W^5 - 9.014 \times 10^{-3}W^4 - 1.574 \times 10^{-3}W^2 \\ + 9.589 \times 10^{-4}W + 3.101 \times 10^{-4}) [(a_4 - 1)W + a_4 + 1] = 0. \end{aligned} \quad (13a)$$

Equation (13a) can be rewritten as

$$\sum_{i=0}^6 A_{4,i} iW^i + \alpha N_1(A_1) \sum_{i=0}^6 A_{1,i} W^i + \beta N_1(A_1) \sum_{i=0}^6 A_{3,i} W^i \times A_{2,i} W^i - N_1(A_1) N_2(A) \cdot K_a N p(t) (1.414 + \alpha + \beta) \sum_{i=0}^6 A_{3,i} W^i = 0. \quad (13b)$$

The real part and imaginary part of Eq. (13) can be found as

$$F_R(V) = \alpha B_1(V) + \beta C_1(V) + D_1(V) = 0 \quad (14a)$$

$$F_I(V) = \alpha B_2(V) + \beta C_2(V) + D_2(V) = 0. \quad (14b)$$

Where B_i, C_i and D_i are functions of A, A_1 and V , Eqs. (14a) and (14b) represent the stability equations of Eq. (13) (5). Now, the problem is to find α, β and A (or A_1) to satisfy Eqs. (12) and (14) for a specified set of values of A (or A_1) and W . The simultaneous solution of Eqs. (12) and (14), i.e. α, β and A (or A_1), shows that a limit cycle may exist.

In the following subsections, the system with one nonlinearity is analysed first, then the system with two nonlinearities is analysed.

IV-1. One nonlinearity in the seeker

After the backlash is replaced by a unit gain, the stability-equation method is applied (6). The results for $K_a = 15$ and $M = 0.2$ are shown in Fig. 7, where the geometry relation $p(t)$ is set at $0.6/N$. In Fig. 7, it can be seen that between the stable region and the unstable region there is a limit cycle region where each point

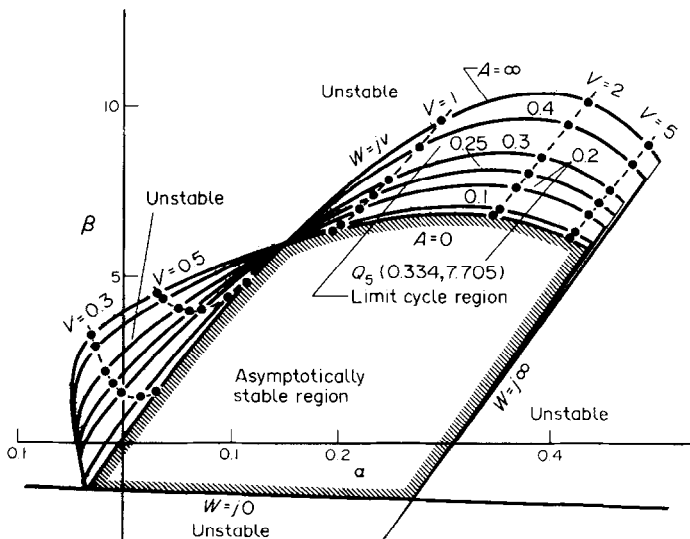


FIG. 7. Limit cycle loci of a nonlinear sampled-data control system with one nonlinearity.

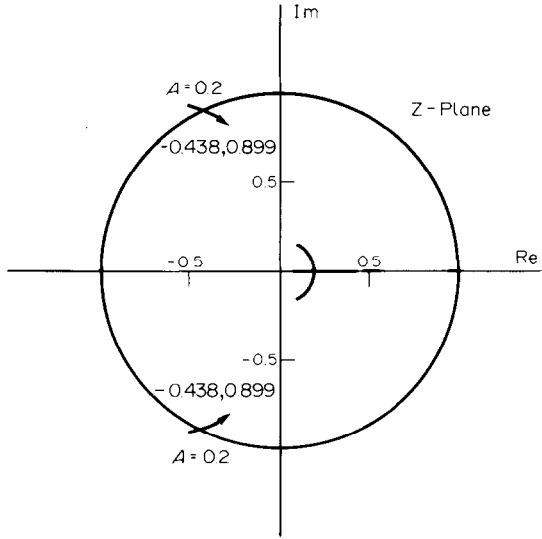


FIG. 8. Roots loci for testing limit cycle stability [$p(t) = 0.6/N$, $\alpha = 0.334$, $\beta = 7.705$].

represents a set of α and β which will make the system have a limit cycle with a certain amplitude and frequency.

In order to check the characteristics of a limit cycle, a point $Q_5 (0.334, 7.705)$ on the curve for $A = 0.20$ in Fig. 7 is selected. Substituting the corresponding values of α and β of Q_5 into Eq. (8a), the characteristic roots near the unit circle in the Z-plane can be found for each value of A . By changing the value of A from $A < 0.2$ to $A > 0.2$, the root loci are given in Fig. 8. It can be seen that Q_5 represents a stable limit cycle

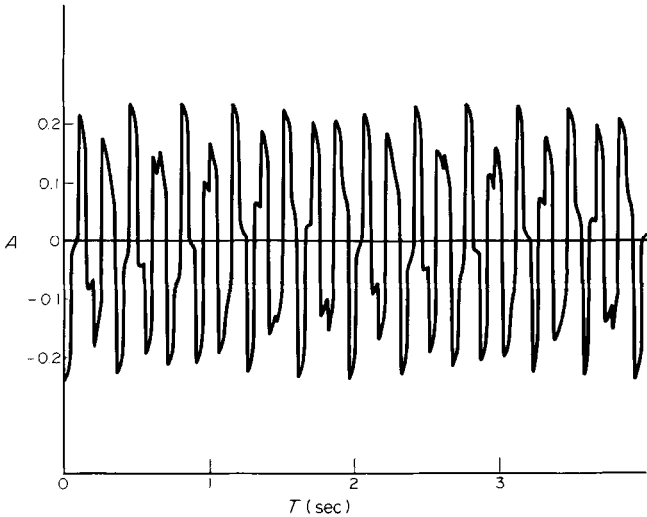


FIG. 9. Limit cycle of a nonlinear sampled-data control system.

with amplitude $A = 0.20$ and $W = 40.488$ (6). By computer simulation the limit cycle represented by Q_5 can be found as shown in Fig. 9.

In Fig. 7, since each point in the limit cycle region will give a limit cycle, several points in this region have been tested, the results are given in Table I. It can be seen that the simulated results are quite close to those found by calculation. For any point above this region, i.e. $A = \infty$, the system is unstable; this implies that the system cannot track the target, because the swing of the seeker diverges to infinity. The regions below the curve for $w = j0$ and above the curve for $A = \infty$ are unstable regions. Note that the stable region of the nonlinear system is smaller than that of the linear system. Note also that a point in the shaded region will be given an asymptotically stable system. This characteristic has also been checked by computer simulation.

IV-2. Two nonlinearities in the system

By applying the same method, the results of the analysis are shown in Figs. 10 and 11 for $K_a = 15$, $M = 0.2$, and $d = 0.05$. Figure 10 shows the results that the reference point (A_1) is selected at the input of the backlash, and Fig. 11 shows those of the reference point (A) selected at the input of the nonlinearity in the seeker.

Figure 10 shows that the shaded area is an asymptotically stable region, and the limit cycle region is below the curve for $A_1 = \infty$ and above the shaded area. A limit cycle represented by Q_6 (0.318, 5.678) can be found as shown in Fig. 12. Several points have also been tested, the results are given in Table II.

The regions outside the shaded area and the limit cycle region are unstable. Note that the stable region of the system with two nonlinearities is smaller than that of the

TABLE I
Theoretical and simulated results of limit cycles

Parameters		Calculated		Simulated	
α	β	A	ω (rad/sec)	A	ω (rad/sec)
0.288	7.033	0.100	38.022	0.197	33.003
0.316	7.079	0.100	40.488	0.066	35.565
0.270	7.451	0.200	35.042	0.278	31.098
0.306	7.652	0.200	38.022	0.243	33.637
0.338	7.705	0.200	40.488	0.197	36.914
0.236	7.381	0.250	31.416	0.296	28.210
0.283	7.879	0.250	35.042	0.229	31.416
0.319	8.094	0.250	38.0219	0.208	34.33
0.250	7.838	0.300	31.416	0.319	28.734
0.297	8.372	0.300	35.042	0.229	32.571
0.359	8.639	0.300	40.488	0.2605	36.545
0.204	7.227	0.350	31.416	0.351	29.613
0.312	8.895	0.350	35.042	0.307	33.339
0.326	9.407	0.400	35.042	0.360	33.408

Q_5

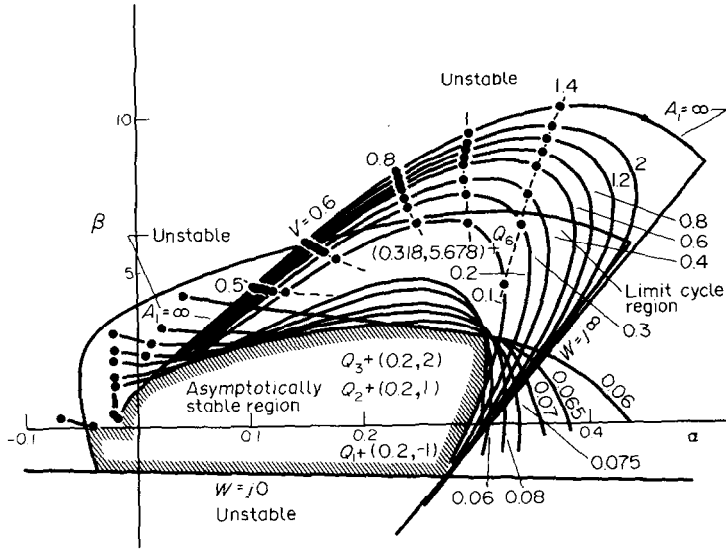


Fig. 10. Limit cycle loci of a nonlinear sampled-data control system with two nonlinearities.

system with one nonlinearity. For the same values of α and β , the limit cycles are greater for the system with two nonlinearities; Figs. 7 and 10 show the differences.

Similarly, three points Q_1 , Q_2 and Q_3 in the asymptotically stable region are selected. The simulated results are given in Figs. 13 and 14, where the magnitude of

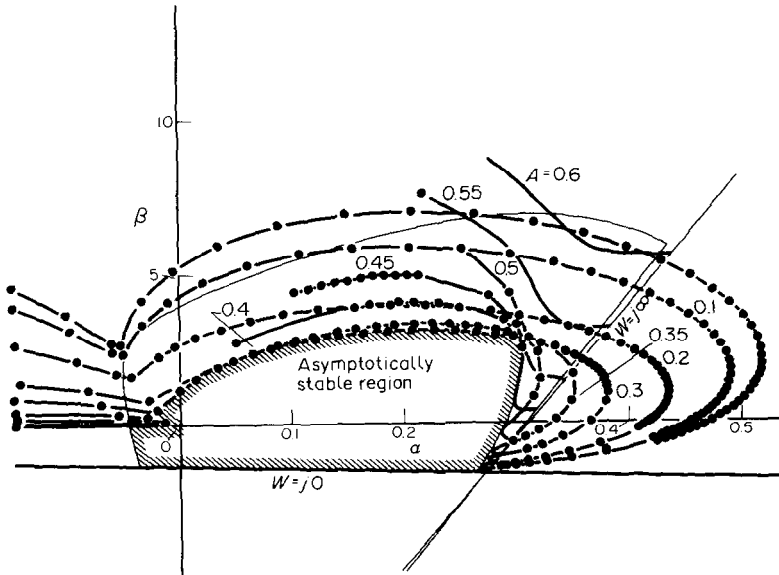


FIG. 11. Limit cycle loci of a nonlinear sampled-data control system with two nonlinearities.

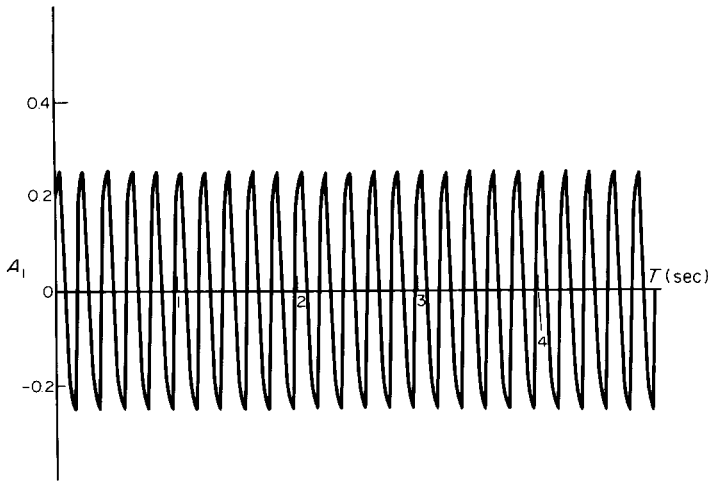


FIG. 12. Limit cycle of a nonlinear sampled-data control system.

the initial disturbance is 0.3, and $p(t)$ set at $0.6/N$ and $0.6 \cos 25t/N$, respectively. Since the signal A dies out quickly, the target is tracked.

From Figs. 2, 3 and 10, it can be seen that for any set of values of α and β , the characteristics of the system are quite different due to the effects of samplers and

TABLE II
Theoretical and simulated results of limit cycles

Parameters		Calculated		Simulated	
α	β	A_1	ω (rad/sec)	A_1	ω (rad/sec)
0.292	-1.145	0.100	35.042	0.106	31.416
0.179	5.399	0.200	21.617	0.415	22.671
0.295	6.452	0.200	31.416	0.472	31.419
0.318	5.678	0.200	35.042	0.254	31.835
0.121	4.352	0.300	18.546	0.414	18.558
0.188	6.042	0.300	23.055	0.470	23.562
0.242	7.034	0.300	26.990	0.526	27.26
0.323	7.173	0.300	35.042	0.591	34.190
0.139	5.039	0.400	20.114	0.651	19.568
0.183	6.159	0.400	23.055	0.597	22.907
0.238	7.286	0.400	26.989	0.625	27.150
0.327	7.866	0.400	35.042	0.628	34.272
0.366	5.434	0.400	44.286	0.440	39.984
0.236	7.439	0.500	36.604	0.763	35.263
0.330	8.547	0.600	35.042	0.886	34.689

Q_6

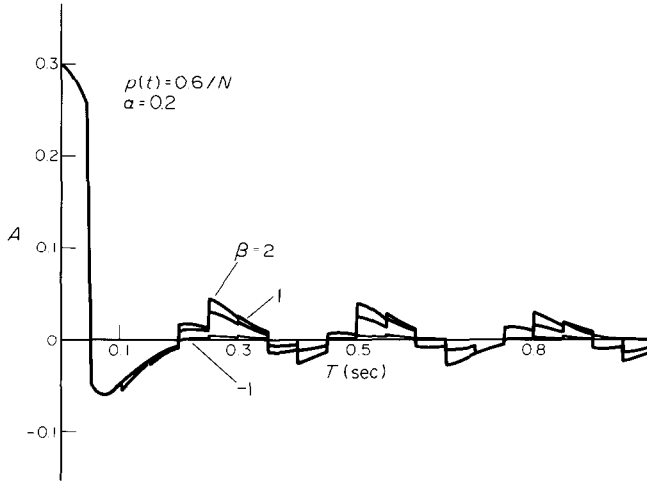


FIG. 13. Responses of a nonlinear sampled-data control system to a testing signal.

nonlinearities. It can be seen also that the method used in this paper can provide a thorough analysis of this rather complicated system.

V. Conclusions

In this paper, the stability-equation method is used to analyse a nonlinear sampled-data proportional navigation system. The stability boundaries, and the limit cycle regions have been found, and checked by computer simulations. In a comparison with the results given in the current literature (3), the results in this

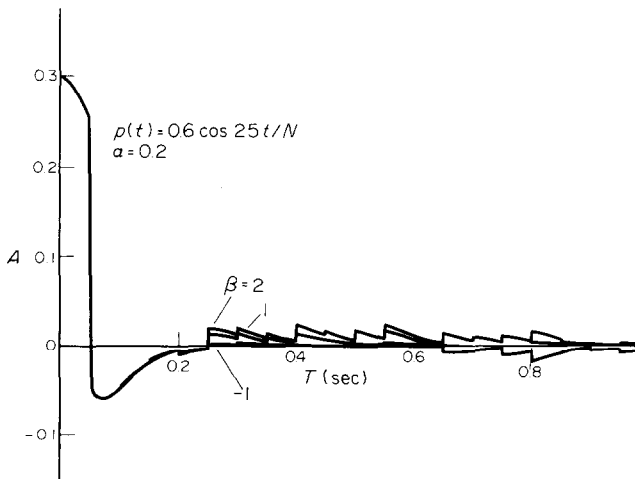


FIG. 14. Responses of a nonlinear sampled-data control system to a testing signal.

paper provide a more thorough understanding of the effects of nonlinearities and their adjustable parameters.

References

- (1) M. Abramowitz, "Theoretical investigation of the performance of proportional navigation guidance system—effect of millile configuration on the speed of response", NACA RM A52J22, Jan. 1953.
- (2) Y. T. Tsay and K. W. Han, "Stability equation method for sampled-data system", *J. Franklin Inst.* Vol. 301, pp. 335–356, April 1976.
- (3) L. C. Wang and K. W. Han, "Analysis of sampled-data control system by stability equation method", *J. Franklin Inst.*, Vol. 306, No. 1, July, 1978.
- (4) D. D. Siljak, "Analysis and synthesis of feedback control system in the parameter plane", *IEEE Trans. Appl. Ind.* Vol. 83, pp. 449–473, Nov. 1964.
- (5) K. W. Han, "Digital and Sampled-data Control Systems", Kuang-Mei, Lungtan, Taiwan, 1979.
- (6) K. W. Han, "Nonlinear Control Systems", Academic Cultural Comp, Box 255, Santa Clara, CA, 1977.

Appendix. Stability Equation Parameter-plane Method (2)

Consider the characteristic equation with complex coefficients

$$F(s) = \sum_{K=0}^n (a_K + jb_K)S^K \quad (\text{A.1})$$

which can be partitioned into real and imaginary parts

$$F_R + F_I = 0 \quad (\text{A.2})$$

where

$$\begin{aligned} F_R &= a_0 + jb_1S + a_2S^2 + kb_3S^3 + \dots \\ F_I &= jb_0 + a_1S + jb_2S^2 + a_3S^3 + \dots \end{aligned} \quad (\text{A.3})$$

The necessary and sufficient condition for the system to be stable is that all the roots of the real part (Z_i) and the imaginary part (p_i) of Eq. (A.3) are on the imaginary axis of the S -plane, and their value is related as

$$\dots Z_{-2} < P_{-1} < Z_{-1} < P_0 < Z_1 < P_1 < Z_2 < \dots \quad (\text{A.4})$$

where P_0 is the origin of the S -plane.

Now consider the coefficients of Eq. (A.1) as a linear combination of variable system parameters α and β as follows:

$$\begin{aligned} a_K &= \alpha c_K + \beta d_K + e_K \\ b_K &= \alpha f_K + \beta g_K + h_K. \end{aligned} \quad (\text{A.5})$$

The complex variable S is replaced by $j\omega$, then Eq. (A.2) can be rewritten as the following expressions:

$$\begin{aligned} F_R(\omega) &= \alpha B_1(\omega) + \beta C_1(\omega) + D_1(\omega) \\ F_I(\omega) &= \alpha B_2(\omega) + \beta C_2(\omega) + D_2(\omega). \end{aligned} \quad (\text{A.6})$$

Equation (A.6) can be solved for unknown α and β

$$\begin{aligned}\alpha &= \frac{C_1(\omega)D_1(\omega) - C_2(\omega)D_1(\omega)}{B_1(\omega)C_2(\omega) - B_2(\omega)C_1(\omega)} \\ \beta &= \frac{B_2(\omega)D_1(\omega) - B_1(\omega)D_2(\omega)}{B_1(\omega)C_2(\omega) - B_2(\omega)C_1(\omega)}.\end{aligned}\tag{A.7}$$

In the α - β plane Eq. (A.7) may represent the locus of points corresponding to the roots with frequency ω . Equation (A.7) represents at least one root of real part and one root of imaginary part equal to $j\omega$. If the roots, except one root of real part and one root of imaginary part, are equal to $j\omega$, and satisfy Eq. (A.3), then a limit cycle may exist.